The Evolution of Ga and As Core Levels in the Formation of Fe/GaAs (001): A High Resolution Soft X-ray Photoelectron Spectroscopic Study

Jamie D. W. Thompson, James R. Neal, Tiehan H. Shen*

Joule Physics Laboratory, Institute for Materials Research, University of Salford, Salford M5 4WT, U.K.

Simon A. Morton, James G. Tobin

Lawrence Livermore National Laboratory, California 94550, U.S.A.

G. Dan Waddill

Physics Department, Missouri University of Science and Technology, Missouri, 65409, USA

Jim A.D. Matthew

Department of Physics, University of York, York YO1 5DD, U.K.

Denis Greig

Department of Physics and Astronomy, University of Leeds, Leeds LS2 9JT, U.K.

Mark Hopkinson

EPSRC National Centre for III-V Technologies, University of Sheffield, Mappin Street, Sheffield, S1 3JD, UK

ABSTRACT

A high resolution soft x-ray photoelectron spectroscopic study of Ga and As 3*d* core levels has been conducted for Fe/GaAs (001) as a function of Fe thickness. This work has provided unambiguous evidence of substrate disrupting chemical reactions induced by the Fe overlayer – a quantitative analysis of the acquired spectra

* Corresponding author, e-mail: t.shen@salford.ac.uk

indicates significantly differing behavior of Ga and As during Fe growth, and our observations have been compared with existing theoretical models. Our results demonstrate that the outdiffusing Ga and As remain largely confined to the interface region, forming a thin intermixed layer. Whereas at low coverages Fe has little influence on the underlying GaAs substrate, the onset of substrate disruption when the Fe thickness reaches 3.5 Å results in major changes in the energy distribution curves (EDCs) of both As and Ga 3*d* cores. Our quantitative analysis suggests the presence of two additional As environments of metallic character; one bound to the interfacial region and another which, as confirmed by *in situ* oxidation experiments, surface segregates and persists over a wide range of overlayer thickness. Analysis of the corresponding Ga 3*d* EDCs found not two, but three additional environments – also metallic in nature. Two of the three are interface-resident whereas the third undergoes outdiffusion at low Fe coverages. Based on the variations of the integrated intensities of each component, we present a schematic of the proposed chemical make-up of the Fe/GaAs (001) system.

I. INTRODUCTION

The prospect of incorporating spin discrimination into microelectronic systems[1,2] has prompted a great deal of interest in the monolithic integration of ferromagnetic metals and semiconductors in recent years. Of these, the Fe/GaAs heterostructure has received the most attention by a significant margin, due in part to the small lattice mismatch (~1.4%) which enables bcc Fe to grow epitaxially upon the zinc-blende crystal structure of GaAs.[3,4] Unfortunately, however, it has been found that the interface of this system deviates somewhat from the 'abrupt' ideal; studies have shown that direct growth of Fe upon GaAs is accompanied by concomitant substrate disruption, resulting in the outdiffusion of As and Ga into the Fe overlayer and the surface segregation of As atoms.[3,5-14] The literature also shows that this dissociation will occur irrespective of reconstruction (be it As-rich or Ga-rich) and growth temperature; these parameters, it seems, influence only the degree of substrate atom incorporation/compound formation observed. These experimental data on the early stages of Fe/GaAs interface development are in good general agreement with the associated theoretical models.[15-17] In a bid to counter substrate disruption, several preventative strategies have been invoked, including the use of buffer layers[13,18,19] and passivation[20,21] of the substrate surface.

The magnetic properties of the Fe/GaAs interface have been studied extensively. For instance, a uniaxial magnetic anisotropy has been observed by many groups for ultra-thin Fe overlayers; a behavior that is strikingly different from the fourfold symmetry associated with bulk bcc Fe (see Ref. 22 for a full review). Moreover, a long-standing subject of considerable interest is the apparent quenching of the magnetization in the first few monolayers (ML) of Fe growth and, indeed, at the film's surface. This reduction, which may be detrimental for spintronic systems,

has been attributed to both 'magnetically dead layers'[23] and 'half-magnetization phases'[24,25] resulting from the intermixing of substrate and overlayer atoms. On the other hand, several groups have demonstrated the absence of such magnetically dead layers when Fe growth is conducted upon As-depleted GaAs surfaces[26-29].

The delayed onset of ferromagnetism in the Fe/GaAs system has also been the subject of intense interest. Various groups have explored this behavior using a variety of techniques and have delivered results for the onset ranging from a few ML up to values as high as 10.5ML.[30-39] Aside from compound formation, it has been suggested that this deferment of ferromagnetic character is heavily dependent on the three-dimensional (3D) growth morphology of the developing Fe overlayer. In an *in situ* study[32] the evolution of the magneto optical Kerr effect (MOKE) signal with Fe coverage was attributed to the existence of a superparamagnetic phase sandwiched between nonmagnetic (below 3.5 ML coverage) and ferromagnetic (4.8 ML +) phases in the growth of Fe films on GaAs at room temperature (RT). Superparamagnetic behavior has not been universally observed, however. In other work,[31,34] observations of a reduction in Curie temperature for ultra thin Fe films on GaAs suggest that this effect, in agreement with the behavior exhibited by ultra thin magnetic films grown on metallic substrates,[40,41] could be the main reason for the absence of a ferromagnetic response at RT.

Whilst excellent studies[3,5--8,13] can be found in the literature wherein photoelectron spectroscopy has been applied with a view to addressing the interfacial chemical environment (and its evolution) during the growth of Fe on GaAs, high resolution work that enables better quantification[42] has been surprisingly sparse[14]. In this work, *high resolution* X-ray photoelectron spectroscopy is utilized to systematically study the Fe/GaAs (001) system as a function of Fe thickness, thus

facilitating quantitative analysis of the interfacial chemical evolution and meaningful comparison of the results to existing theoretical models. We present clear evidence of substrate disrupting chemical reactions induced by the overlayer, in addition to the segregation of an As species whose surface residency is confirmed by the approach of *in situ* oxidation.

II. EXPERIMENTAL

The Fe/GaAs growth results presented herein were obtained at the 'Spin Chamber' endstation of Beamline 7.0.1 at the Advanced Light Source (ALS), Berkeley using Soft X-ray Photoemission Spectroscopy (SXPS), whereas the oxidation study was conducted during a separate run at the 'Electronic Structure Factory' endstation of the same beamline.

The substrates considered in this study were prepared at the III-V facility at The University of Sheffield and consisted of highly doped n-type GaAs epilayers grown upon singular n^+ GaAs (001) substrates and capped with amorphous As. The capped substrates were then relocated to the appropriate ALS endstation (see above), where clean GaAs (001) surfaces with a range of Ga:As ratios (see Table I) were prepared *in situ* by thermal desorption ('decapping') of the capping layer. Fe was then sequentially deposited by e-beam evaporation at a rate determined by a quartz crystal oscillator to be ~ 1 Å/min. The same procedure had been employed in earlier in-house experimental work[43], where clear patterns of low energy electron diffraction were observed from both the decapped substrates and the Fe films subsequently deposited, suggesting well ordered surface structures.

Between each deposition step of the growth study (conducted at the Spin Chamber endstation), the sample was transferred from the growth position to the

analysis position for scanning; this process involved both vertical and angular translations and necessitated the use of an additional normalization step if core level intensities for different Fe thicknesses were to be compared. By analogy, for the oxidation study (Electronic Structure Factory endstation), a sample would undergo a relocation between exposure steps. Here, after each exposure, the sample was transferred from the growth chamber through an ultra high vacuum link to the SXPS chamber for analysis, before being returned for further treatment.

In both cases, Energy Distribution Curves (EDCs) for the evolving Fe/GaAs interface were obtained at a chamber pressure better than 3×10^{-10} mbar using a surface sensitive photon energy of 120 eV. Typically, survey scans were taken in the binding energy (BE) range 70 to -5 eV, thereby incorporating all peaks under scrutiny in a single sweep. Energy resolutions for the two endstations were estimated by measuring the energy period over which the Fermi edge of a thin Au film rose from 10 % – 90 % of its maximum value. In this way, a *total* energy resolution (i.e. encompassing thermal and instrumental broadening, as well as the effects of the finite bandwidth of the beamline's photons) of ~ 150 meV was determined for both experimental setups.

III. DATA PROCESSING AND PEAK DECONVOLUTION METHODOLOGY

All data were normalized to the incident photon flux (I_0) and then re-normalized to unity at 44 eV (As 3*d*) or 25 eV (Ga 3*d*). The first step, normalizing to I_0, is a point-by-point beam intensity normalization which filters out any effects arising from variations in beam intensity during the course of the scan. In the absence of an internal reference point, the second normalization step, a 'global' normalization, was requisite in order to circumvent the effects of *external* influences

upon the measured intensities (e.g. the variation of sample position between deposition cycles) and thereby facilitate quantitative intensity comparisons across multiple spectra. Although this procedure operates under the premise of a constant secondary background (which is not necessarily the case), unphysical trends are only observed if this step is omitted. Finally, for purposes of presentation alone, each data set was normalized to the total integrated intensity of the associated clean bulk substrate.

Subsequent to the application of the aforementioned normalizations, empirical curve fitting was performed on each spectrum using commercially available software ('CASAXPS', Casa Software Ltd.). After removal of a Tougaard background, the compound As 3*d* and Ga 3*d* lineshapes were decomposed into a number of synthetic spin-orbit (SO) split doublets by employing a 'minimum components' philosophy and ensuring that the requirement of self-consistency amongst all data was fulfilled.[44] Phonon/instrumental broadening and core-hole lifetime contributions to the detected signals were accounted for by approximating the Voigt function (a lineshape formed by the convolution of Gaussian and Lorentzian distributions) by a linear Gaussian-Lorentzian (GL) mix of the form

$$S(E) = \eta\left[1 + 4\left(\frac{E - E_0}{\gamma}\right)^2\right]^{-1} + (1-\eta)\exp\left[-4\ln 2\left(\frac{E - E_0}{\gamma}\right)^2\right] \quad (1)$$

where η is the fractional weight of the Lorentzian contribution, E is the energy and E_0 and γ represent the centroid and Full-width-at-Half Maximum (FWHM) of the whole function, respectively.

Where necessary, loss processes resulting in asymmetric broadenings (e.g. screening resulting from electron-hole pair formation) were modeled by the Doniach-Sunjic (DS) function

$$Y(E) = \frac{\Gamma(1-\alpha)}{\left[(E-E_0)^2 + 4\gamma^2\right]^{(1-\alpha)/2}} \cos\left\{\frac{\pi\alpha}{2} + (1-\alpha)\arctan\left(2\left(\frac{E-E_0}{\gamma}\right)\right)\right\} \quad (2)$$

where Γ is the gamma function, α is the asymmetry parameter, E is defined as in Eq. 1 and E_0 and γ represent the centroid and FWHM of the unskewed Lorentzian (i.e. the lineshape to which the DS function reduces when the asymmetry parameter, α, is set to zero). Although DS functions convoluted with Gaussians (to account for instrumental/phonon broadening) have been shown to model the lineshapes associated with electron emission from *pure metals*[45] rather well, we found that, despite repeated attempts, this was not the case for the metal/semiconductor system considered in this work: here, such an approach appeared to lead to an unacceptably poor quality of fit on the low BE side of each peak. Therefore, an alternative, pragmatic approach was adopted wherein–the line-shape to the low BE side of the peak maximum was represented by the Voigt approximation (as before) and the behavior on the high BE side was fitted with a pure DS function convoluted with a Gaussian. The asymmetry of the lineshape generated by such a hybrid function is characterized by the asymmetry index a:

$$a = 1 - \frac{FWHM_{left}}{FWHM_{right}} \quad (3)$$

where $FWHM_{left}$ and $FWHM_{right}$ are the Full-Width-at-Half-Maximum values to the left (high BE side) and right (low BE side) of the peak position. The procedure, albeit *ad hoc*, appeared to provide a much better fitting quality (the reasons for its success, however, are a subject for future investigation). Furthermore, fitting procedures with linear and Shirley types of background have also been used, yielding similar results. We therefore are reassured that the spectroscopic features of interest identified in the present work are reasonably reliable.

The SO splittings used for the As- and Ga-derived components were determined from analysis of the clean substrate EDCs and fixed for the entirety of each series. The theoretical relative intensity ('branching ratio') between $3d_{3/2}$ and $3d_{5/2}$ states of 2:3 was also introduced as a fixed parameter. FWHM and asymmetry values for the synthetic doublets not originating from the bulk substrate were determined from consideration of every EDC in each series and held rigidly for every fit, whereas no restrictions were imposed upon the peak positions or intensities. The fixing of the FWHM and asymmetry parameters was found to be essential if physically sensible intensity variations of peaks fitted with the DS line-shape were to be achieved.

All BE shifts in this work are expressed relative to the position of the associated bulk substrate component according to

$$shift_{(X)} = BE_{(X)} - BE_{(bulk)} \quad (4)$$

where $shift_{(X)}$ is the amount by which component 'X' is shifted relative to the appropriate bulk-derived signal; and $BE_{(X)}$ and $BE_{(bulk)}$ are the BEs of the component in question and the substrate component, respectively.

IV. RESULTS AND DISCUSSION

The ensuing sections present and discuss the results of the current work. A brief discussion of the substrate surfaces utilized in this study is presented first (Section A), followed by, in Section B, a general description of the overall trends, coupled with elementary descriptions of the outcomes resulting from deconvolution of the As and Ga 3*d* core levels observed at various stages of Fe growth. Thereafter, more detailed analyses of the data corresponding to interface-resident (Section C) and out-diffused/segregated (Section D) species are presented. In Section E, each

chemical environment determined from the deconvolution is categorized. Drawing from the results detailed in the preceding segments, the proposed chemical make-up of the Fe/GaAs system is introduced in Section F.

A. Substrate Spectra

In total, four GaAs (001) substrates, decapped under nominally identical conditions and henceforth labeled A – D, were utilized for the core level evolution study presented herein. Our strategy was to grow different thicknesses of Fe on each surface and then interlace the resulting spectra to form a single, generalized picture of the core level evolution with increasing Fe thickness. Our purpose here was twofold: to confirm the reproducibility of the collected data and, secondly, *to demonstrate the insensitivity of the observed trends to the precise details of the initial GaAs surface*. In Fig. 1(a) we present an example wide scan (70 to -5 eV), acquired subsequent to decapping of Substrate D, wherein the success of the decapping procedure, and thereby the provision of a clean GaAs surface, is confirmed by the absence of an O 2*s* signal. Further ratification of cleanliness was also provided by inspection of spectra acquired over the energy range: 1000 to -5 eV (not shown).

Spectra acquired after decapping each of the four substrates are presented in Fig. 2 and the associated fitting parameters, determined from the minimization, are provided in Table I. The As:Ga ratios are also listed in Table I. Two surface-shifted components, one either side of those associated with the 'bulk' GaAs matrix, are typically present for both the As 3*d* and Ga 3*d* cores. Substrate B, having the smallest As:Ga ratio of the set, differs in that there is no sign of the high BE surface component (typically attributed to surface-resident As dimers) which is clearly visible in the spectra of the other three. This may suggest that substrate B had considerable

As depletion at its surface. These spectra are in excellent agreement with those obtained from earlier works with similar substrates.[46--49]

B. Core Level Evolution with Fe Growth

In Fig.1, the overall behavior observed for the As 3*d*, Ga 3*d* and Fe 3*p* core levels, as well as the evolution of the valence band, during Fe growth on Substrate D is presented for selected stages of Fe deposition (clean substrate, 7.5, 30 and 50 Å). Whereas a signal originating from the As 3*d* core level is clearly detected for all coverages presented, the Ga 3*d* line, by contrast, undergoes rapid attenuation with increasing Fe thickness and is no longer observable beyond a coverage of 30 Å. Meanwhile, as expected, the deposition of Fe leads to the appearance of the Fe 3*p* line and a concomitant enhancement of emission from the valence band. The appearance of an additional valence band feature at ~3 eV below the Fermi level in the higher coverage spectra (30 and 50 Å of Fe coverage) is indicative of the onset of bulklike ferromagnetic band structure in the Fe film (further details of this effect will be published elsewhere).

EDC evolution with Fe thickness for the deconvoluted As 3*d* and Ga 3*d* core levels is depicted in Figs. 3 and 4, respectively, and the fitting parameters for the Fe-induced components are listed in Table II. Peak intensities determined from the deconvolution process are plotted in Figs. 5 (As 3*d* core) and 6 (Ga 3*d* core).

After 2 Å of Fe deposition, referring to Figs. 3 and 4, we note rather little change in the shape of the core level spectra of either substrate element. However, the fits reveal enhancements in the intensities of the As(s-I) and Ga(s-I) lines, in addition to shifts in the binding energies of the As(s-II) and Ga(s-II) components (moving from +0.59 to +0.81 eV and from +0.72 to +0.88 eV, respectively). Close

inspection of the Ga core line reveals a slight swing in spectral weight towards lower binding energy.

Increasing the Fe coverage to 3.5 Å leads to the disappearance of the surface-related components and the arrival of new reacted-phase signals for both As and Ga 3*d* core levels. Considering first the As 3*d* core, the EDC can be deconstructed into three distinct chemical environments: one originating from the bulk substrate and an additional two characterized by binding energies similar to those of the surface-shifted components observed for the clean substrate. The larger of these two components, labeled As(I), is shifted by -0.51 eV and the other, As(II), is shifted by +0.74 eV relative to the BE of the bulk-derived doublet. The FWHM values for these two components were determined by the minimization to be 0.54 eV – only slightly lower than that observed for the bulk substrate (0.6 eV). Examination of the Ga 3*d* core reveals yet further evidence of Fe-induced substrate disruption. Here, the two surface-shifted components have been replaced by three reacted-phase signatures: two shifted to binding energies lower than that of the bulk and a third component shifted to higher binding energy. The peak exhibiting the greatest shift to lower BE (-0.9 eV) has been labeled Ga(I) and is the weakest of the trio at this coverage. Adjacent to this, designated Ga(II), lies the strongest of the new arrivals, located approximately halfway between Ga(I) and the bulk-derived component (-0.43 eV shift). Ga(III), on the other hand, is shifted in the opposite sense, with a +0.75 eV shift. The minimization determined the FWHM values for these components to be 0.38 eV [Ga(I)), 0.55 eV (Ga(II)) and 0.6 eV (Ga(III)].

The deposition of a further 3 Å of Fe (6.5 Å in total) leads to sizeable changes in the lineshapes of both the As 3*d* and Ga 3*d* core levels: the As 3*d* core has developed a well-defined shoulder on the low BE side of the EDC and two clear

shoulders can be observed on the same side of the Ga 3*d* spectrum. The structural change of the As 3*d* EDC can be attributed to a marked increase in the intensity of the As(I) doublet and the concomitant decrease of the signal intensity from the bulk substrate (Fig. 5). Having peaked at a coverage of 3.5 Å, the intensity of the As(II) component has already started to attenuate. Moving over to the Ga 3*d* lineshape, we note with reference to Fig. 6 that the structural development taking place on the low BE side of the spectrum is largely owing to the strengthening of the Ga(I) signal partnered with the attenuation of the Ga(II) and substrate-derived components. Similar to the As(II) case, components Ga(II) and Ga(III) appear to have reached their maximum intensities after only 3.5 Å of Fe deposition.

As the Fe coverage is further increased, the As 3*d* EDC is evermore dominated by the As(I) signal as the As(II) doublet continues to diminish in magnitude and the bulk substrate signal decays with the expected exponential behavior. As(I) sharply strengthens until around 7.5 – 9 Å of Fe coverage, where it peaks and is thereafter attenuated. The rate of attenuation is low, however, and the intensity remains significant even after 100 Å of Fe have been deposited. As(I) is the only As-derived component detectable for coverages of 30 Å and above.

Turning now to the Ga 3*d* core, we found a behavior not too dissimilar from that observed for the As 3*d* case. Here, the Ga(I) signal is enhanced until it peaks at a coverage of around 7.5 – 9 Å. This component is, however, subsequently attenuated until it disappears for coverages greater than 30 Å. Having passed through their intensity maxima at a coverage of 3.5 Å, the Ga(II) and Ga(III) signatures become undetectable for coverages above 17 Å. In tandem with the As-derived bulk substrate component, the bulk signal from the Ga core weakens at an exponential rate and vanishes at the same thickness as the Ga(II) and Ga(III) lines do.

C. Interface Development

The evolvement of the *total* integrated intensities of the As and Ga 3*d* EDCs, accompanied by the theoretical intensity variation (assuming the absence of outdiffusion, layer-by-layer Fe growth and an attenuation length of 6 Å) is plotted in Fig. 7. Referring first to Figs. 3 and 4, we note that the spectral shape of the As and Ga *3d* cores is not altered by any sizeable degree after 2 Å of Fe deposition and, also, that both EDCs could be fitted by employing components similar in character to those used for the bare substrate fits. A gentle swing of spectral weight towards the low BE side of the Ga 3*d* spectrum is, however, observed and we shall return to this point later. For greater coverages (3.5 Å +), on the other hand, the nature of the components required in the fitting changes dramatically – this behavior indicates that no drastic level of substrate disruption occurs for coverages below the 3.5 Å mark. Examination of the total integrated intensity variations with Fe thickness (Fig. 6) lends further credence to this model: for coverages below 3.5 Å the experimentally determined intensities of both core levels follow closely those predicted if negligible substrate disruption and two-dimensional growth is assumed. Beyond this thickness, the As signal rapidly veers away from the predicted path before reaching a fairly constant (albeit diminishing) level for thicknesses above 17 Å. The behavior of the Ga signal closely mimics that of the 'no diffusion' model for coverages below 12.5 Å, before exhibiting a reduced rate of attenuation.

In an earlier study, Kneedler *et al.*[8] attributed the character of the levels at low coverage (≤ 2 ML: 1 ML = ~ 1.5 Å) to the transference of charge (as opposed to Fe-induced substrate disruption) based on the constancy of the As 3*d* lineshape and the identification of a newly-developed bias in spectral weight towards the low BE side of

the Ga 3*d* EDC – a behavior closely followed by the results of this work. Considering the thermodynamics of the system, the heats of formation ΔH of the structurally congruent reacted phases (Fe_2As: -38 kJ/mol, Fe_2Ga: -16 kJ/mol) dictate that the Fe adatoms will preferentially bond to the As members of the GaAs matrix.[5] Taking this to be the case, and incorporating the respective Pauling electronegativities of each element in the picture (Fe: 1.83, As: 2.18, Ga: 1.81),[5] one may speculate that the observed increase in charge on the surface Ga atoms is a direct result of the breaking of Ga-As bonds, driven by the system's forestalling of the relatively undesirable Fe-Ga bond. Using this straightforward thermodynamic argument, coupled with the experimental data, it has been hypothesised[8] that the arrival of Fe atoms leads to the 'stripping away' of Ga and As substrate atoms (and their subsequent incorporation into the overlying Fe film) until an interface exclusively composed of Fe-As bonds can be formed. We note here that the unavailability of a complete layer of As atoms for GaAs (110) substrates has been attributed to the predominantly 3D growth mode and higher population of defects observed for this particular surface.[50]

This simple argument is augmented by the theoretical work of Erwin, Lee and Scheffler.[15] Using density-functional theory, they were able to model the nucleation and growth of Fe on GaAs (001) ranging from the submonolayer regime to coverages of several monolayers. Their calculations predicted that upon the initial arrival of Fe adatoms (i.e. < 1 ML coverage), the preference for high Fe co-ordination and the relative energetic favorability of Fe-As heterodimers would lead to intermixing by the breaking of Ga dimers (present for Ga-terminated surfaces) and Ga-As surface bonds.

For coverages between 1 and 2 ML, they identified a termination-dependent transition of interface morphology wherein abrupt interfaces are favored for As-terminated GaAs and 'virtually abrupt' (slightly intermixed) interfaces become

energetically desirable for the Ga-terminated variant (such termination dependent interface morphologies have also been predicted by the calculations of Demchenko and Liu[16]). They showed that this change was the result of a shift in the relative benefit of achieving maximal Fe co-ordination and minimizing the excess population of interfacial Fe from the former to the latter. In agreement with the simple thermodynamic model outlined above, this would lead to the 'kicking out' of top layer substrate atoms and the creation of an interface ideally monopolized by Fe-As bonding. This model (hereafter referred to as the 'Erwin model') cannot be reconciled with the results of the present study, however. As presented in Figs. 3 and 4, our analysis of Fe growth upon As-rich, and therefore most likely As-terminated, GaAs surfaces implies substantial intermixing at the Fe/GaAs interface: our curve-fitting reveals the presence of three lines [As(I), Ga(II) and Ga(III)] whose intensities peak after only 3.5 Å of Fe have been deposited and whose interface residency is demonstrated by their attenuation rates, which match those of the bulk substrate components. Whilst it is appreciated that the amount of weight which can be attached to the comparatively weak, high BE components [As(II) and Ga(III)] is debatable owing to the inexactness of the background removal process, some justification for their inclusion can be gleaned from the fact that their presence was also found to be requisite when other background types were employed (linear and Shirley). Regardless, it is suggested that the presence of Ga(II) is sufficient in itself to discount the existence of the abrupt Fe-As dominated interface predicted by the Erwin model.

A study by Mirbt *et al.*[17] (henceforth referred to as the 'Mirbt model') also finds disagreement with the Erwin model on this issue: this group, having taken the energetic effects of surface segregation into account, found that As and Ga outdiffusion will occur irrespective of termination and that an intermixed interface is

always a lower energy configuration than its abrupt counterpart. Their prediction was vindicated in part by the work of Kneedler *et al.*[8] who found that outdiffusion of Ga was still present for the Fe/GaAs (001)-*c*(4×4) system – this system consists of 0.75 ML of As dimers atop a full monolayer of As. In this case the Erwin model (and the simple thermodynamic considerations outlined earlier) differs from experiment in that it would not predict any Ga outdiffusion, as no bulk substrate bonds would have to be broken in order to achieve the energetically desirable planar Fe-As interface. The results of the present study also seem to follow the pathway set out by the Mirbt model, finding agreement on both key points: in addition to the presence of three interface resident components, our work has also pointed to Ga outdiffusion [component Ga(I)]. Accordingly, we propose the existence of an interfacial, intermixed Fe-Ga-As phase; as predicted by the aforementioned Mirbt model.

D. Surface Segregation

The segregation of an As species to the Fe surface in the Fe/GaAs system was first detected in the XPS studies of Waldrop and Grant,[3] and this observation has since been ratified by several authors,[3,5--14] but not all.[23] The energetic implications of the presence of substrate-derived adlayers during Fe growth have also been explored in the theoretical works of Erwin *et al.*[15] and Mirbt *et al.*[17].

In agreement with these earlier studies, the presence of a segregated As phase in the present work is clearly evidenced by the persistence of an As-derived SXPS line, As(I), up to Fe coverages of 100 Å (the highest coverage under consideration). Any suggestion that this component may originate from the bulk substrate is precluded by the absence of an accompanying Ga line. That this segregated component is single phase is made clear by the core level deconvolution, in which

only a single DS doublet is required for the provision of a good fit (as discussed in Section B).

In order to ascertain whether the segregated As resides in surface or sub-surface sites, we monitored the As 3*d* EDC as an Fe (100 Å)/GaAs (001) sample was sequentially exposed to varying doses of oxygen – the premise here being that the creation of an As_xO_y species would imply that the As is resident in the vicinity of the surface region of the Fe/GaAs system. Here, we allowed for the disorder the oxide brings to the system by freeing the previously fixed FWHM parameter. The results of this experiment are illustrated in Fig. 8. At zero exposure, the As 3*d* core consists of only a single SO-split doublet, earlier designated As(I), with a FWHM of 0.54 eV. 20 langmuirs (L) of exposure to O_2 leads to a 41 % broadening of As I to 0.76 eV and the arrival of an additional, broad doublet (hereafter labeled 'As(O)' and possessing a FWHM of 0.91 eV at this point) shifted by 2.61 eV relative to the substrate position. After exposure to a further 50 L of O_2 (70 L in total), the strength of the reacted doublet had become comparable to that of As(I). In this spectrum, the FWHM of As(I) narrowed slightly to 0.71 eV whilst that of As(O) further increased to 1.05 eV. Whilst little change was evident after exposure to a further 100 L, the subsequent addition of a further 200 L (totaling 370 L) led to a complete inversion in spectral weight in favor of the oxide. After this degree of oxidation, the continued reduction in the FWHM of component As(I) was found to persist, whereas that of As(O) remained at a steady value of 1.05 eV.

Although the exposures utilized in this study were insufficient to fully oxidize the As 3*d* line, we believe it is clear that a conversion to the oxide approaching 100 % is readily achievable. Accordingly, we conclude that the vast majority, if not the entirety, of the intensity observed from the As 3*d* line originates from surface-

segregated As, providing a separate confirmation of that reported previously. Although not presented, the evolution of the Fe 3*p* core level was also monitored and was observed to oxidise in tandem with the As 3*d* signal. This behaviour, it is speculated, arises owing to the incompleteness of the segregated As layer.[13]

The experimentally observed GaAs substrate dissociation (owing to the addition of an Fe overlayer) and the ensuing surface segregation of As atoms are in excellent agreement with the predictions of the appropriate theoretical works. Erwin *et al*,.[15] in their model, have shown that the surface energy of the Fe/GaAs (001) system is significantly reduced in the presence of a substrate-derived adlayer (be it As or Ga) riding on the surface – this outcome was found to stand irrespective of Fe film thickness or the details of the GaAs termination. The lack of discrimination with regard to surface termination is in good general agreement with our observation of the presence of As surface segregation for Fe grown on either As- or Ga-rich surfaces. Mirbt *et al.*[17] furthered this in their calculations, finding that As surface segregation is not at all dictated by diffusion (it does, in fact, depend upon chemical bonding) and that the process will take place even at extremely low temperatures. Additionally, they found that Ga also has a tendency to surface-segregate, but that this process, which must be thermally activated, will be inhibited by the surface segregating As atoms. Our results, in good agreement with this study, appear to show that Ga atoms do indeed segregate (the signal from this phase, as indicated in Figs. 6 and 7, persists far longer than that of the associated bulk-substrate component, indicating some degree of segregation), but that this outdiffusion process is only short-lived and the reacted Ga remains 'locked' in close proximity to the interface with increasing Fe coverage. Interestingly, both segregating layers [As(I) and Ga(I)] reach their intensity maxima at a coverage in the vicinity of 7.5-9 Å with As(I) being the much stronger of

the two. In light of this, we believe that, up to coverages of 7.5-9 Å, both As and Ga atoms surface segregate in order to reduce the surface energy and that, beyond this coverage, the presence of the segregated As precludes any further Ga segregation. This proposal is supported by similar work on the analogous Ni/GaAs (110) system[51]. Further support for this notion of As and Ga co-segregation during the growth of Fe on GaAs is also provided by the Auger Electron Spectroscopy (AES) studies of Sano and Miyagawa – here, however, Ga segregation was observed only for high growth temperatures.[7]

In other work, Sano and Miyagawa also found that if the surface-riding atoms are removed by sputter etching, the adlayer does not make a reappearance, even if the sample is annealed.[52] This behavior indicated that, after the initial segregation step, the population of the segregating layer continues to re-segregate to the surface *during* Fe deposition, and is not fed/replenished by atoms from the substrate or overlying film: a deposition-concurrent surface segregation (DCSS). In their model of DCSS, the authors propose that the segregated atoms are never buried more than 1 ML beneath the surface and that *all* of the segregated atoms will eventually re-segregate upon the arrival of newly deposited atoms. This, they cite as a cyclical surface energy minimization process. With reference to Fig. 5, we note that the results of the present study do not fall in line with this 'total re-segregation' mechanism proposed by Sano and Miyagawa: it is clear from this figure that the intensity of the segregated As component, As(I), exhibits a linear decay for coverages of 30 Å and above – weakening at a rate just below 5 % per 10 Å between Fe thicknesses of 30 and 100 Å. Assuming that this monotonic decrease in intensity persists to higher coverages, a linear extrapolation predicts that all of the segregated As will be consumed by the Fe film once a coverage of ~ 240 Å is reached.

E. Assignment of Chemical Environments

Although the precise categorization of deconvoluted XPS peaks is typically beset by ambiguity, such an endeavor can nevertheless be a fruitful exercise. Referring to an analogous high resolution study conducted by Ludge *et al.*[42] we note that our core level evolution results bear a striking resemblance, in form at least, to those obtained for Co grown on the As-rich GaAs (001) *c*(4×4) reconstructed surface. For growth at a substrate temperature of 150 °C, they observed the formation of three As-derived reacted phases, two (which they labeled As-I_1 and As-I_2) shifted to binding energies lower than that of bulk coordinated As, and one (As-S) shifted to higher binding energy. The presence of two Ga-derived reaction products (Ga-I_1 and Ga-I_2) was also noted, and both were found to be characterized by shifts to binding energies lower than that of the Ga-As bonding typifying the bulk. For low coverages (2 ML), a very weak (undesignated) component shifted to high BE can also be seen.

The most significant differences between the spectra from the Co study and those considered in this article are twofold. Firstly, considering the As 3*d* core, the Co/GaAs spectra have an additional, albeit weak, low BE component that is not seen in our corresponding Fe/GaAs spectra. Given that the surface sensitivities and resolutions of the two studies are comparable, it is unlikely that experimental constraints are responsible for the absence of this component in the current work. We note, however, that the much higher substrate temperature used for the Co growth may have facilitated the arrangement of an additional bonding configuration not accessible at the growth temperatures employed in this study. The second obvious difference is found in the character of the Ga 3*d* core – this time the Fe/GaAs spectra have an additional high binding energy component. We tentatively attribute this

discrepancy to the fact that the *c*(4×4) surface is rather Ga impoverished relative to the surface used in our work.

In order to establish the origins of the observed peaks, the authors[50] grew CoAs and CoGa films atop clean GaAs (001) *c*(4×4) surfaces and observed shifts of 0.5 and 1 eV, respectively, to binding energies lower than those of the bulk. The CoAs shift was very similar to that of component As-I_2 and, accordingly, this doublet was attributed to the formation of a CoAs-like phase. By analogy, we classify our segregated (or 'floating') As-derived component, As(I), as an FeAs-like environment. The peak resulting from the deposition of CoGa was shifted to a binding energy 1 eV below that of the bulk substrate – a shift comparable in magnitude to that of Ga-I_1. In line with this, Ga-I_1 was attributed to the formation of a CoGa-like phase. The spectral evolution and shift of Ga(I) accurately mimics that of Ga-I_1 and we thereby attribute it to the signature of an FeGa-like compound (in line with Schultz and co-workers[13]).

As described in Section B, components As(II), Ga(II) and Ga(III) all reach their intensity maxima after only 3.5 Å of Fe deposition and are thereafter attenuated, finally becoming undetectable at the same thickness as the bulk-derived components (~17 Å +). Accordingly, it is clear that the bonding environments responsible for these lines are interface-resident, reaching no further than a few Å into the overlying Fe film. The model of Mirbt *et al.*[17] suggests that intermixed interfaces generally provide the lowest energy bonding configuration and we suggest that these three lines originate from an intermixed Fe-Ga-As containing phase which sits within a few Å of the substrate/overlayer interface.

F. Proposed Structure

Based on the variations of the integrated intensities of each component, and the considerations discussed in sections 4.3 – 4.5, we present a schematic of the proposed chemical make-up of the Fe/GaAs (001) system in Fig 9. Close to the interface, in the first few Å, the chemical interplay between the Fe adatoms and the underlying substrate matrix appears to result in the formation of an intermixed Fe-Ga-As phase, though the precise stoichiometry of this phase has not been determined in this work. Beyond this layer (extending approximately 7.5 – 9 Å from the overlayer-substrate interface) exists an FeGa-like phase resulting from a reaction between 'kicked-out' Ga atoms and the overlying Fe film. After this layer lies a bulklike Fe phase which contains small quantities of material 'lost' from a segregating layer of As during each resegregation step. Finally, riding on the Fe film is a dwindling layer of As in an FeAs-like environment.

V. SUMMARY

Our high resolution SXPS study of the ultra high vacuum (UHV) growth of Fe upon GaAs (001), combined with in-situ oxidation experiments, has provided unambiguous evidence that substrate disrupting chemical reactions and As surface-segregation are induced during deposition of the Fe overlayer and, consequently, has facilitated the proposal of a simple model describing the overall chemical structure of this system. Our proposed structure consists of: an intermixed Fe-Ga-As phase, and an FeGa-like region, whose combined thickness is no greater than 9 Å; a thick layer of bulklike Fe containing small quantities of As; and, finally, a thin FeAs-like phase resulting from the continual, but 'lossy', surface segregation of As atoms during Fe growth. The relatively sharp nature of the reacted interface implied by the model

suggests that Fe/GaAs grown at ambient temperatures may, after all, be a suitable candidate for inclusion in future spintronic device applications.[53]

ACKNOWLEDGEMENTS

We acknowledge gratefully the support from the UK Engineering and Physical Sciences Research Council (EPSRC) and travel grants from the University of Salford. Both J.D.W. Thompson and J.R. Neal would like to thank the EPSRC for their research studentship. We also wish to thank Prof. E.A. Seddon for her involvement in the early part of this work, Dr. N. Fairley and Prof. N. Takahashi for useful discussions, Dr. J. Zhang for her assistance in the preparation of the graphs, and, finally, Prof. P.J. Grundy for his interest in this work and his valued encouragement. This work was performed under the auspices of the U.S. Department Of Energy (DOE) by the University of California, Lawrence Livermore National Laboratory (LLNL) under Contract No. W-7405-Eng-48. Work by LLNL personnel was funded in part by the Office of Basic Energy Science at DOE. The ALS and the Beamline 4 Spectromicroscopy Facility have been built and operated under funding from the Office of Basic Energy Science at DOE.

REFERENCES

[1]S.Datta and B.Das, Appl. Phys. Lett. **56**, 665 (1990).

[2]G.A. Prinz, Science **282**, 1660 (1998).

[3]J.R. Waldrop and R.W. Grant, Appl. Phys. Lett. **34**, 630 (1979).

[4]G.A. Prinz and J.J. Krebs, Appl Phys Lett. **39**, 397 (1981).

[5]M.W. Ruckman, J.J. Joyce and J.H. Weaver, Phys. Rev. B. **33**, 7029 (1986).

[6]S.A. Chambers, F. Xu, H.W. Chen, I.M. Vitomirov, S.B. Anderson and J.H. Weaver, Phys. Rev. B **34**, 6605 (1986).

[7]K. Sano and T. Miyagawa, Jap. J. Appl. Phys. **30**, 1434 (1991).

[8]E. Kneedler, P.M. Thibado, B.T. Jonker, B.R. Bennett, B.V. Shanabrook, R.J. Wagner and L.J. Whitman, J. Vacuum Science and Technology B **14**, 3193 (1996).

[9]E.M. Kneedler, B.T. Jonker, P.M. Thibado, R.J. Wagner, B.V. Shanabrook and L.J. Whitman, Phys. Rev. B **56**, 8163 (1997).

[10]T.L. Monchesky, B. Heinrich, R. Urban, K. Myrtle, M. Klaua and J. Kirschner, Phys. Rev. B **60**, 10242 (1999).

[11]T. Manago, M. Mizuguchi and H. Akinaga, J. Cryst. Growth **237-239**, 1378 (2002).

[12]R. Moosbuhler, F. Bensch, M. Dumm and G. Bayreuther, J. Appl. Phys. **91**, 8757 (2002).

[13]B.D. Schultz, H.H. Farrell, M.M.R. Evans, K. Lu¨ dge and C.J. Palmstrøm, J. Vac. Sci. Tech. B **20**, 1600 (2002).

[14]C.M. Teodorescu and D. Luca, Surf. Sci. **600**, 4200 (2006).

[15]S.C. Erwin, S.-H. Lee and M. Scheffler, Phys. Rev. B **65**, 205422 (2002)

[16]D.O. Demchenko and A.Y. Liu Phys. Rev. B **73**, 115332 (2006)

[17]S. Mirbt, B. Sanyal, C. Isheden and B. Johnson, Phys. Rev. B **67**, 155421 (2003).

[18]Y. Chye, V. Huard, M.E. White and P.M. Petroff, Appl. Phys. Lett. **80**, 449 (2002).

[19]T. Zhang, M. Spangenberg, N. Takahashi, T.-H. Shen, D. Greig, J.A.D. Matthew and E.A. Seddon, Appl. Surf. Sci. 191, 211 (2002).

[20]G.W. Anderson, M.C. Hanf and P.R. Norton, Phys. Rev. Lett. **74**, 2764 (1995).

[21]A. Filipe and A. Schuhl, J. Appl. Phys. **81**, 4359 (1997).

[22]G. Wastlbauer and J.A.C. Bland, Adv. in Phys. **54**, 137 (2005).

[23]J.J. Krebs, B.T. Jonker and G.A. Prinz, J. Appl. Phys. **61**, 2596 (1987).

[24]A. Filipe, A. Schuhl, and P. Galtier, Appl. Phys. Lett. **70**, 129 (1997).

[25]A. Filipe and A. Schuhl, J. Appl. Phys. **81**, 4359 (1997).

[26]M. Zolfl, S. Kreuzer, T. Schweinbock, M. Brockman, M. Kohler, S. Mietaner, F. Bensch and G. Bayreuther, J. Magn. Magn. Mater. **175**, 16 (1997).

[27]Y.B. Xu, M. Tselepi, E. Dudzik, C. M. Guertler, C.A.F. Vaz, G. Wastlbauer, D.J. Freeland, J.A.C. Bland and G. van der Laan, J. Magn. Magn. Mater. **226**, 1643 (2001).

[28]M. Doi, B. Roldan Cuenya, W. Keune, T. Schmitte, A. Nefedov, H. Zabel, D. Spoddig, R. Meckenstock and J. Pelzl, J. Magn. Magn. Mater. **240**, 407 (2002).

[29]B. Roldan Cuenya, M. Doi, W. Keune, S. Hoch, D. Reuter, A. Wieck, T. Schmitte and H. Zabel, Appl. Phys. Lett. **82**, 1072 (2003).

[30]M. Gester, C. Daboo, R.J. Hicken, S.J. Gray, A. Ercole and J.A.C. Bland, J. Appl. Phys. **80**, 347 (1996).

[31]M. Spangenberg, J.R. Neal, T.-H. Shen, S.A. Morton, J.G. Tobin, G.D. Waddill, J.A.D. Matthew, D. Greig, A.E.R. Malins, E.A. Seddon and M. Hopkinson J. Magn. Magn. Mater. **292**, 241 (2004).

[32]Y. B. Xu, E.T.M. Kernohan, D.J. Freeland, A. Ercole, M. Tselepi, and J.A.C. Bland, Phys. Rev. B **58**, 890 (1998).

[33]D.J. Freeland, Y.B. Xu, E.T.M. Kernohan, M. Tselepi and J.A.C. Bland, Thin Sol. Films **344**, 210 (1999)

[34]F. Bensch, G. Garreau, R. Mossbuhler, G. Bayreuther and E. Beaurepaire, J. Appl. Phys. **89**, 7133 (2001).

[35]S.J. Steinmuller, M. Tselepi, V. Strom and J.A.C. Bland, J. Appl. Phys. **91**, 8679 (2002).

[36]T. Zhang, N. Takahashi, M. Spangenberg, T.-H. Shen, E.A. Seddon, D. Greig and J.A.D. Matthew, Appl. Surf. Sci. **193**, 217 (2002).

[37]J.S. Claydon, Y.B. Xu, M. Tselepi, J.A.C. Bland and G. van der Laan, J. Appl. Phys. **95**, 6543 (2004).

[38]J. Herfort, W. Braun, A. Trampert, H.-P. Schönherr and K. H. Ploog, Applied Surface Science **237**, 181 (2004).

[39]M. Madami, S. Tacchi, G. Carlotti, G. Gubbiotti and R.L. Stamps, Phys. Rev. B **69** 144408 (2004).

[40]S.D. Bader, J. Magn. Magn. Mater. **100**, 440 (1991).

[41]P. Poulopoulos and K. Baberschke, J.Phys.: Condens. Matter **11**, 9495 (1999).

[42]K. Ludge, B.D. Schultz, P. Vogt, M.M.R. Evans, W. Braun, C.J. Palmstrom, W. Richter and N. Esser, J. Vac. Sci. Technol. B **20**, 1591 (2002).

[43]Y. Liu, Ph.D. Thesis, University of Salford (2005).

[44]J.J. Joyce, M. Del Giudice and J.H. Weaver, J. Elec. Spect. Rel. Phenom. **49**, 31 (1989).

[45]P.H. Citrin, G.K. Wertheil and Y. Baer, Phys. Rev. B **16**, 4256 (1977).

[46]A.D. Katnani, H.W. Sang, Jr., P. Chiaradia and R.S. Bauer, J. Vac. Sci Technol. B **3**, 608 (1984)

[47]G. Le Lay, D. Mao, A. Kahn, Y. Hwu and G. Margaritondo, Phys. Rev. B **43**, 14301 (1991).

[48]I.M. Vitomirov, A. Raisanen, A.C. Finnefrock, R.E. Viturro, L.J. Brillson, P.D. Kirchner, G.D. Pettit and J.M. Woodall, Phys. Rev. B **46**, 13293 (1992).

[49]M. Marsi, R. Houdre, A. Rudra, M. Ilegems, F. Gozzo, C. Coluzza and G. Margaritondo, Phys. Rev. B **47**, 6455 (1993).

[50]H.-P. Schonherr, R. Notzel, W. Ma and K.H. Ploog, J. Appl. Phys. **89**, 169 (2001).

[51]M.D. Williams, W.G. Pedro, T. Kendelewicz, S.H. Pan, I Lindau and W.E. Spicer, Sol. Stat. Comm. **51**, 819 (1984).

[52]K. Sano and T. Miyagawa, Appl. Surf. Sci. **60/61**, 813 (1992).

[53]R. Sato and K. Mizushima, Appl. Phys. Lett. **79**, 1157 (2001).

Figure captions:

FIG. 1. Representative wide scan SXPS spectra (hυ = 120 eV) obtained from Substrate D at selected stages of Fe growth: (a) prior to deposition (clean substrate), (b) 7.5 Å, (c) 30 Å and (d) 50 Å.

FIG. 2. Curve-fitted SXPS spectra of the As 3*d* (left) and Ga 3*d* (right) EDCs after thermal desorption of the capping layer.

FIG. 3. The evolution of the As 3*d* core level with increasing Fe coverage for the Fe/GaAs (001) system. After 2 Å of Fe growth, the surface components observed for the 'bare' substrate are still visible. For greater coverages (3.5 Å +), the onset of substrate disruption leads to the arrival of metallic 'reacted' components As(I) and As(II). Once a coverage of 30 Å is reached only the component originating from surface-segregated As (As(I)) is observed.

FIG. 4. The evolution of the Ga 3*d* core level with increasing Fe coverage for the Fe/GaAs (001) system. By analogy with Fig. 3, no signs of significant chemical reactivity after 2 Å of Fe have been deposited. For coverages between 3.5 Å and 12.5 Å, these components have been replaced by 3 lines related to metallic 'reacted' Ga though their number is reduced to 2 when the coverage is increased to 17 Å. Once a coverage of 30 Å is reached, only a single, outdiffused component (Ga(I)) remains; though this line, too, vanishes when the coverage is further increased.

FIG. 5. Plot of integrated intensity *vs.* Fe thickness for the deconvoluted As 3*d* components. For clarity, eye-guiding curves have been added to the plot such that the general trends are highlighted. Whereas the bulk substrate component is reduced with the expected exponential decay, component As(II) undergoes a peak in intensity after only 3.5 Å of Fe have been deposited, before vanishing in tandem with the bulk substrate line. Having peaked between 7.5 and 9 Å of Fe coverage, the As(I) line is still detectable at the highest coverage studied (100 Å).

FIG. 6. Plot of integrated intensity *vs.* Fe thickness for the deconvoluted Ga 3*d* components. For clarity, eye-guiding curves have been added to the plot such that the general trends are highlighted. Note also the change of scale on the ordinate axes as compared with that of Fig.5. In the likeness of the As 3*d* case, the bulk substrate components decays with the expected exponential behavior. Whereas component Ga(I) shows clear signs of out-diffusion, components Ga(II) and Ga(III) are confined to the interfacial region.

FIG. 7. The variation of the total integrated intensities with Fe thickness for the As and Ga 3*d* core levels. Also included in the plot is the predicted intensity 'drop-off' if the absence of out-diffusion, layer-by-layer Fe growth and an attenuation length of 6 Å are assumed. Whilst the Ga signal closely follows the theoretical decay up to coverages in excess of 10 Å, the As signal rapidly veers away from this 'unreactive interface' picture after only a few Å of Fe deposition.

FIG. 8. The effect of increasing levels of O_2 exposure on the As 3*d* EDC obtained from a sample of the form Fe (100 Å)/GaAs (001). The initial dose of O_2 (20 L)

results in the arrival of an oxidized As component. After a dose of 175 L the relative intensities of the two peaks are inverted and, by 375 L (the greatest exposure used), the oxide-derived peak dominates the EDC.

FIG. 9. (Color online). Schematic diagram of the chemical structure of the Fe/GaAs (001) system after 100 Å of Fe growth; the structure of which is based in the intensity variations of the deconvoluted Ga and As 3*d* components. An outdiffused FeGa-like phase sits between an intermixed interfacial region and 'bulklike' Fe; above which rides a thin layer of segregated As in an FeAs-like environment.

Substrate		A	B	C	D
BE shift (eV)	As(s-I)	-0.51	-0.51	-0.53	-0.52
	As(s-II)	0.57	…	0.71	0.55
	Ga(s-I)	-0.43	-0.44	-0.41	-0.41
	Ga(s-II)	0.75	0.83	0.65	0.62
FWHM (eV)	As(bulk)	0.57	0.59	0.59	0.56
	As(s-I)	0.57	0.59	0.59	0.56
	As(s-II)	0.71	…	0.70	0.69
	Ga(bulk)	0.51	0.52	0.51	0.49
	Ga(s-I)	0.51	0.52	0.51	0.49
	Ga(s-II)	0.57	0.55	0.65	0.72
As:Ga ratio		1.60	1.27	1.33	1.53

Table I: Binding Energy shift (BE shift), Full-Width-at-Half-Maximum (FWHM) and As to Ga ratio (As:Ga ratio) parameters concerning the four substrates used for the core level evolution study.

		As(I)	As(II)	Ga(I)	Ga(II)	Ga(III)
FWHM (eV)		0.54	0.54	0.38	0.55	0.60
	Relative binding energy shift (eV)					
Fe coverage (Å)	3.5[(A)]	- 0.46	+ 0.77	- 0.89	- 0.42	+ 0.79
	6.5[(A)]	- 0.47	+ 0.74	- 0.96	- 0.47	+ 0.80
	7.5[(B)]	- 0.46	+ 0.74	- 0.85	- 0.51	+ 0.58
	7.5[(C)]	- 0.38	+ 0.66	- 0.93	- 0.50	+ 0.82
	9[(B)]	- 0.42	+ 0.75	- 0.89	- 0.47	+ 0.83
	9[(C)]	- 0.46	+ 0.69	- 0.93	- 0.47	+ 0.83
	12.5[(C)]	- 0.36	+ 0.75	- 0.98	- 0.44	+ 0.84
	17[(C)]	- 0.20	+ 1.07	- 0.98	- 0.49	+ 0.84
	17[(D)]	- 0.29	+ 0.83	- 0.87	.	.
	30[(D)]	- 0.09	.	.	.	.
	50[(D)]	- 0.05	.	.	.	.
	100[(D)]	- 0.07	.	.	.	.

	As 3*d*	Ga 3*d*
Spin-orbit splitting	0.69	0.44
Branching ratio	1.5	1.5
Asymmetry index	0.07	0.1

Table II: Full-Width-at-Half-Maximum (FWHM) and relative binding energy shift parameters for the reacted As and Ga components (present for coverages of 3.5 Å and above). The superscripted letters in brackets (left-most column of the table) indicate which substrate was used (A, B, C or D) for each Fe coverage (see Table I for details of the parameters associated with each substrate).

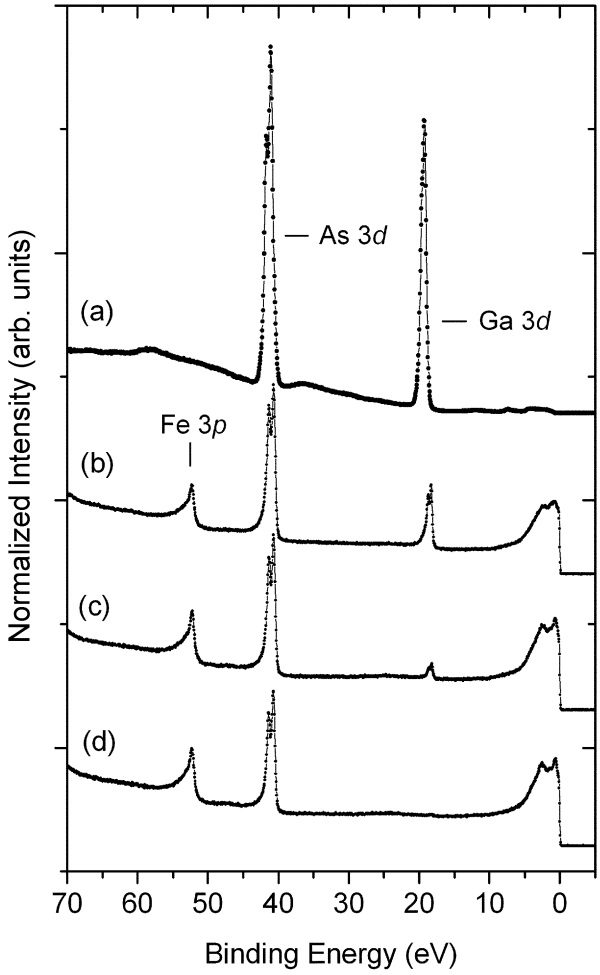
Normalized Intensity (arb. units)
— As 3d
— Ga 3d
(a)
Fe 3p
(b)
(c)
(d)
70
60
50
40
30
20
10
0
Binding Energy (eV)

Figure 1

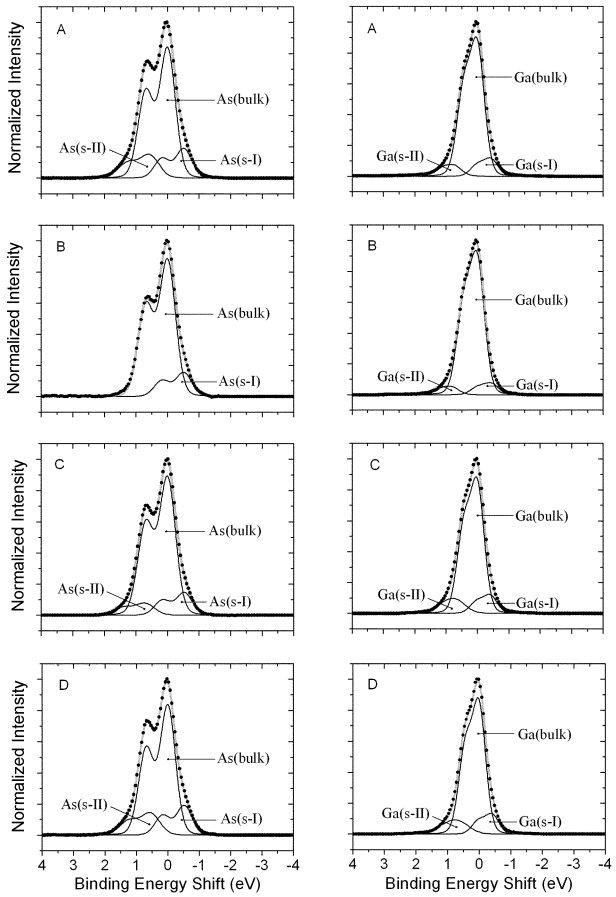
A
As(bulk)
As(s-II)
As(s-I)
Ga(bulk)
Ga(s-II)
Ga(s-I)
B
C
D
Normalized Intensity
4 3 2 1 0 -1 -2 -3 -4
Binding Energy Shift (eV)

Figure 2

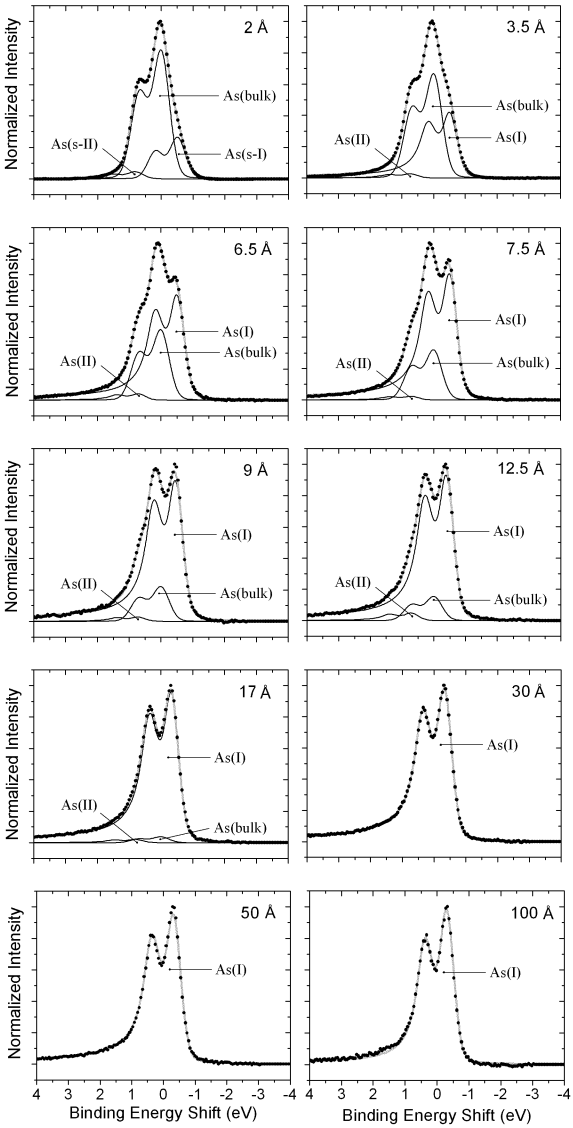
2 Å
As(bulk)
As(s-II)
As(s-I)
3.5 Å
As(bulk)
As(II)
As(I)
6.5 Å
As(I)
As(II)
As(bulk)
7.5 Å
As(I)
As(II)
As(bulk)
9 Å
As(I)
As(II)
As(bulk)
12.5 Å
As(I)
As(II)
As(bulk)
17 Å
As(I)
As(II)
As(bulk)
30 Å
As(I)
50 Å
As(I)
100 Å
As(I)
Normalized Intensity
4 3 2 1 0 -1 -2 -3 -4
Binding Energy Shift (eV)

Figure 3

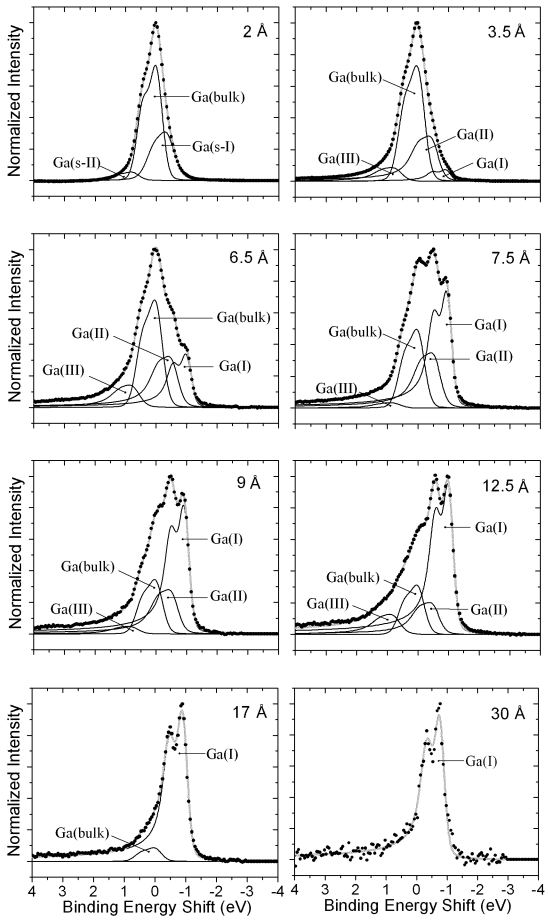
2 Å
Ga(bulk)
Ga(s-I)
Ga(s-II)
3.5 Å
Ga(bulk)
Ga(II)
Ga(III)
Ga(I)
6.5 Å
Ga(II)
Ga(bulk)
Ga(III)
Ga(I)
7.5 Å
Ga(bulk)
Ga(I)
Ga(II)
Ga(III)
9 Å
Ga(I)
Ga(bulk)
Ga(III)
Ga(II)
12.5 Å
Ga(I)
Ga(bulk)
Ga(III)
Ga(II)
17 Å
Ga(I)
Ga(bulk)
30 Å
Ga(I)
Normalized Intensity
4 3 2 1 0 -1 -2 -3 -4
Binding Energy Shift (eV)

Figure 4

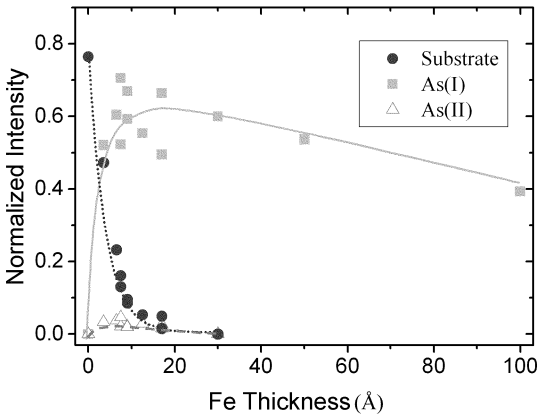
Normalized Intensity
Fe Thickness (Å)
Substrate
As(I)
As(II)
0.0
0.2
0.4
0.6
0.8
0
20
40
60
80
100

Figure 5

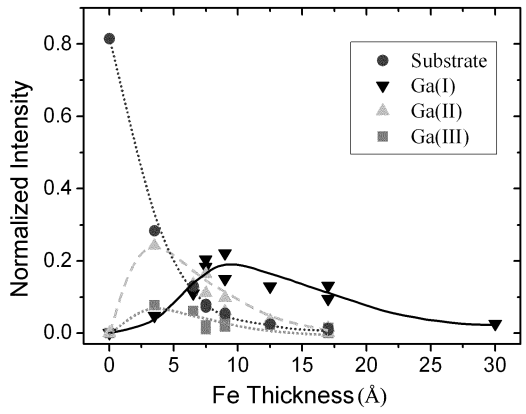
Normalized Intensity
0.0
0.2
0.4
0.6
0.8
0
5
10
15
20
25
30
Fe Thickness (Å)
Substrate
Ga(I)
Ga(II)
Ga(III)

Figure 6

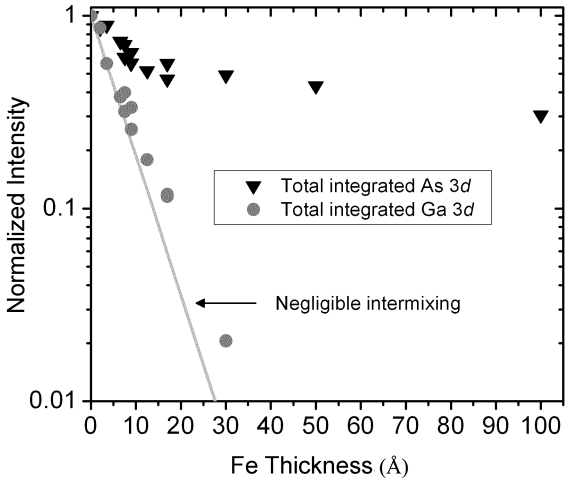
Normalized Intensity
1
0.1
0.01
0
10
20
30
40
50
60
70
80
90
100
Fe Thickness (Å)
Total integrated As 3d
Total integrated Ga 3d
Negligible intermixing

Figure 7

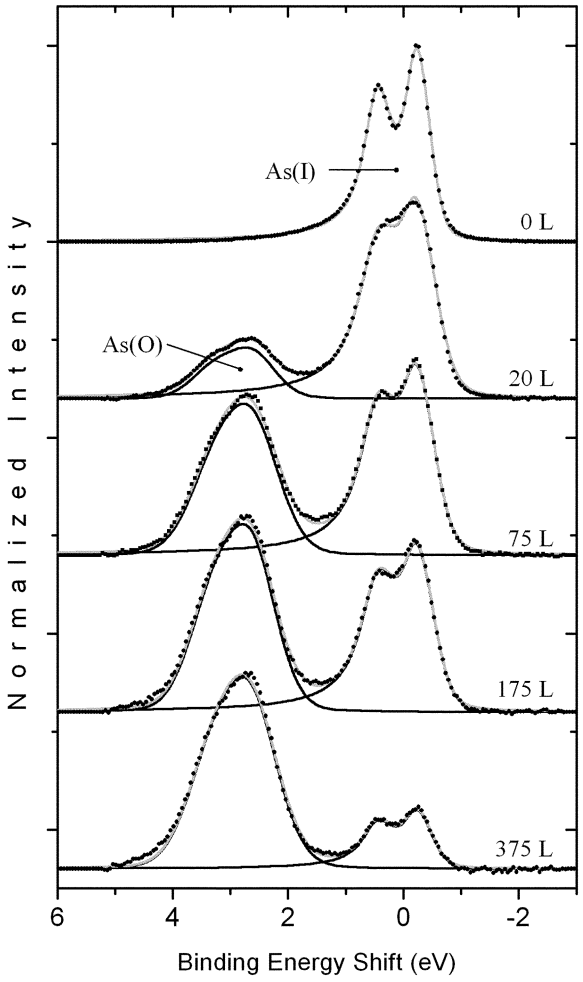
As(I)
0 L
As(O)
20 L
75 L
175 L
375 L
Normalized Intensity
6
4
2
0
-2
Binding Energy Shift (eV)

Figure 8

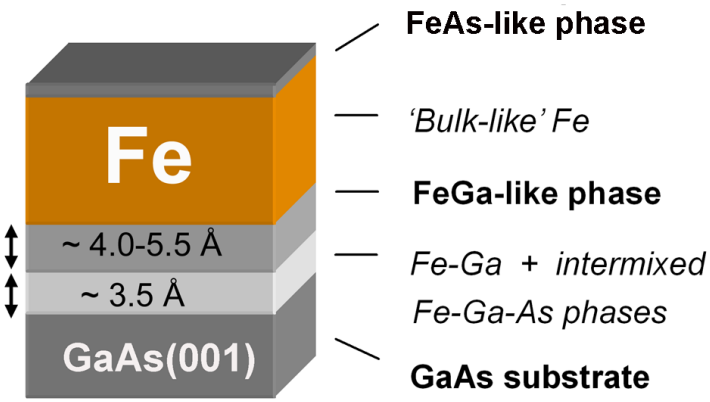
FeAs-like phase
Fe
'Bulk-like' Fe
FeGa-like phase
~ 4.0-5.5 Å
Fe-Ga + intermixed
~ 3.5 Å
Fe-Ga-As phases
GaAs(001)
GaAs substrate

Figure 9